

A GALACTIC CENTER ORIGIN FOR HE 0437–5439, THE HYPERVELOCITY STAR NEAR THE LARGE MAGELLANIC CLOUD¹

WARREN R. BROWN¹, JAY ANDERSON², OLEG Y. GNEDIN³, HOWARD E. BOND², MARGARET J. GELLER¹, SCOTT J. KENYON¹, AND MARIO LIVIO²

¹Smithsonian Astrophysical Observatory, 60 Garden St, Cambridge, MA 02138

²Space Telescope Science Institute, 3700 San Martin Dr., Baltimore, MD 21218

³Department of Astronomy, University of Michigan, Ann Arbor, MI 48109

2010, *ApJ Letters*, 719, L23

ABSTRACT

We use *Hubble Space Telescope* imaging to measure the absolute proper motion of the hypervelocity star (HVS) HE 0437–5439, a short-lived B star located in the direction of the Large Magellanic Cloud (LMC). We observe $(\mu_\alpha, \mu_\delta) = (+0.53 \pm 0.25(\text{stat}) \pm 0.33(\text{sys}), +0.09 \pm 0.21(\text{stat}) \pm 0.48(\text{sys}))$ mas yr⁻¹. The velocity vector points directly away from the center of the Milky Way; an origin from the center of the LMC is ruled out at the 3- σ level. The flight time of the HVS from the Milky Way exceeds its main-sequence lifetime, thus its stellar nature requires it to be a blue straggler. The large space velocity rules out a Galactic-disk ejection. Combining the HVS's observed trajectory, stellar nature, and required initial velocity, we conclude that HE 0437–5439 was most likely a compact binary ejected by the Milky Way's central black hole.

Subject headings: Galaxy: center — Galaxy: stellar content — Galaxy: kinematics and dynamics — (galaxies:) Magellanic Clouds — stars: individual (HE 0437–5439)

1. INTRODUCTION

Hypervelocity stars (HVSs) are stars escaping the Milky Way. Predicted by Hills (1988) as a natural consequence of the massive black hole (MBH) in the Galactic center, HVSs were first discovered by Brown et al. (2005). The proposed ejection mechanism is a three-body interaction between binary stars and a MBH, or possibly a pair of MBHs (Yu & Tremaine 2003), that ejects HVSs from the Milky Way at a rate of 10⁻³ to 10⁻⁴ yr⁻¹ (Perets et al. 2007). Approximately 5% of HVS ejections should be compact binaries (Lu et al. 2007; Perets 2009b). At least 14 unbound stars have now been discovered in a targeted survey for HVSs (Brown et al. 2006a,b, 2007a,b, 2009) and another 3-5 unbound stars discovered in other surveys (Edelmann et al. 2005; Hirsch et al. 2005; Heber et al. 2008; Tillich et al. 2009; Irrgang et al. 2010). Unlike high proper-motion pulsars, which are the remnants of supernova explosions, known HVSs are mostly B-type main-sequence stars (Fuentes et al. 2006; Bonanos et al. 2008; López-Morales & Bonanos 2008; Przybilla et al. 2008a,b). Similar B stars are observed in short-period orbits around the central MBH (Ghez et al. 2008; Gillessen et al. 2009) and may be the former companions of HVSs (Gould & Quillen 2003; Ginsburg & Loeb 2006). But, until now, the evidence linking HVSs to the Galactic center has been indirect.

One of the most intriguing HVSs is HE 0437–5439 (Edelmann et al. 2005), called HVS3 in the catalog of Brown et al. (2009). HVS3 is a 9 M_⊙ B star located 16° from LMC on the sky. It has a heliocentric radial velocity of +723 km s⁻¹ and a heliocentric distance of

61 kpc. The flight time of HVS3 from the Milky Way is about 100 Myr, substantially more than its $\simeq 20$ Myr main-sequence lifetime. Edelmann et al. (2005) consider the possibility that HVS3 was ejected from the Milky Way as a binary and evolved into a 9 M_⊙ blue straggler, but conclude that an ejection from the LMC is more likely.

An LMC origin requires that HVS3 was ejected at nearly 1000 km s⁻¹ (Przybilla et al. 2008a), a velocity comparable to the ~ 1000 km s⁻¹ escape velocity from the surface of the 9 M_⊙ star. Gualandris & Portegies Zwart (2007) suggest that an intermediate-mass black hole (IMBH) in a massive young LMC star cluster can provide the required ejection velocity without disrupting the star. Alternatively, Gvaramadze et al. (2008, 2009) suggest that HVS3 was ejected by a stellar binary-binary encounter involving >100 M_⊙ stars. The full space motion of HVS3 constrains its origin.

We use the *Hubble Space Telescope* (*HST*) to measure the absolute proper motion of HVS3, the first result from an astrometric campaign to measure proper motions for all HVSs. The velocity vector of HVS3 points directly from the Galactic center. Summing the random and systematic proper motion errors, an origin from the center of the LMC is ruled out at the 3- σ level. We bring to bear three observations to restrict the origin of HVS3: its trajectory, stellar nature, and required initial velocity. We rule out a Galactic-disk ejection, and conclude that HVS3 was once a binary ejected by the Milky Way's central MBH as proposed by Perets (2009b).

2. PROPER MOTION

We measure the proper motion of HVS3 using two epochs of *HST* Advanced Camera for Surveys (ACS) imaging obtained on 2006 Jul 8 and 2009 Dec 23. Each epoch consists of six dithered $\simeq 5$ min exposures in the F850LP filter, designed to maximize the signal of the

wbrown@cfa.harvard.edu, jayander@stsci.edu, ognedin@umich.edu

¹Based on observations with the NASA/ESA *Hubble Space Telescope* obtained at the Space Telescope Science Institute, which is operated by the Association of Universities for Research in Astronomy, Inc., under NASA contract NAS5-26555.

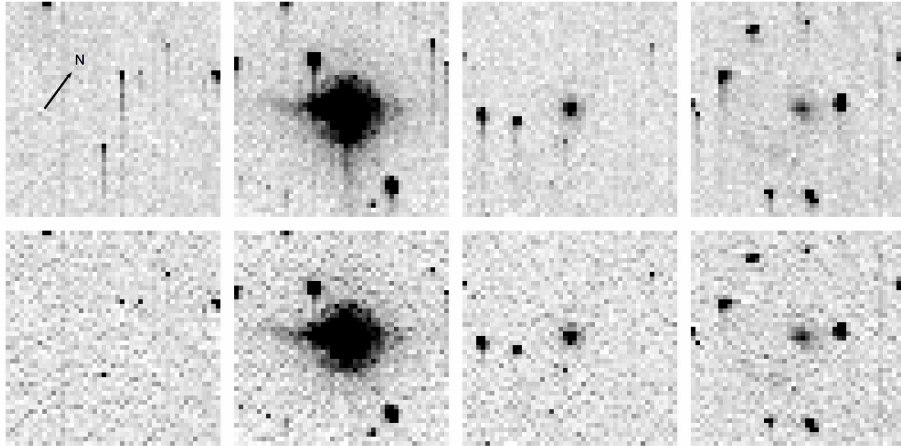


Figure 1. Top row: Uncorrected thumbnail images from epoch-2 showing, from left to right, warm pixels, a bright star, a faint star, and a faint galaxy. CTI trails in the (vertical) readout direction are present in all objects. Bottom row: Corrected images, showing CTI trails restored to their rightful pixels. Readnoise is slightly amplified because the CTI correction is a mild deconvolution, but this adds very little random error to the astrometry.

background galaxies and to prevent the bright HVS from saturating.

Charge-transfer inefficiency (CTI) is the largest source of uncertainty in our proper motion measurement. Physically, CTI is due to pixel defects temporarily trapping electrons as they are shifted across the detector during readout. The consequence is image distortion (seen in Figure 1): up to 20% of a background galaxy’s electrons can be trailed across neighboring pixels in the readout direction (Anderson & Bedin 2010). We can minimize the effects of CTI by obtaining images at the same telescope orientation, but unfortunately our epoch-2 images had to be rotated by 180° relative to our epoch-1 images because the epoch-1 guidestars were no longer available. This mis-orientation magnifies the CTI effect and requires that we correct for it.

We use a pixel-based CTI correction recently developed by Anderson & Bedin (2010). Application of this technique to a 47 Tuc field demonstrates that it mitigates CTI errors to better than 75% in terms of photometry, astrometry, and shape. Figure 1 illustrates the results of CTI correction in one of our epoch-2 images. We apply 55% of the epoch-2 CTI correction to the epoch-1 images, because ACS had been in space about half as long. A study of the warm pixels in dark frames contemporaneous to epoch-1 validates this strategy. If we perform no correction for known CTI effects, we would measure the wrong location for HVS3: its displacement would shift 1.8 mas yr^{-1} north and 1.2 mas yr^{-1} east.

We begin our astrometric measurement by stacking the epoch-2 images, using bright stars to transform the six exposures into a common distortion-corrected frame (Anderson & King 2006). We supersample this frame 2 times relative to the ACS pixel scale. We select 17 stars and 18 compact galaxies and use their stacked images as templates. The templates enable us to measure a consistent position for each object in each exposure (see Mahmud & Anderson 2008). We then define an absolute frame with north up, east on the left, and a scale of 50 mas pix^{-1} . We use the pipeline `drz` images from epoch-1 to measure rough positions for each galaxy and, using the galaxies alone, we determine the transformation from the distortion-corrected frame (Anderson &

King ISR/ACS 04-15) of each exposure into this absolute reference frame. We refine the reference frame and the transformations by taking the average transformed galaxy positions as the new galaxy positions and iterating. A few iterations yield a set of 11 high-quality galaxies with RMS position errors $<12 \text{ mas}$ in the reference frame and $<18 \text{ mas}$ residuals in each individual frame where they are well measured.

We base our final astrometric transformations exclusively on the positions of the 11 high-quality galaxies; thus inter-epoch displacements in our reference frame correspond directly to HVS3’s absolute proper motion. Figure 2 plots the 36 displacements found from comparing each of the six epoch-1 images against each of the six epoch-2 images. The average displacement is $0.0375 \pm 0.017 \text{ pix}$ over the 3.46 yr baseline, which corresponds to $(\mu_\alpha, \mu_\delta) = (+0.53 \pm 0.25, +0.09 \pm 0.21) \text{ mas yr}^{-1}$. Here we quote the $1\text{-}\sigma$ error-in-the-mean, calculated under the conservative assumption that there are 6 independent epoch-1 – epoch2 differences. As a check, we compute HVS3’s displacement using two bright galaxies directly east and west of the object and find an answer consistent at the $1\text{-}\sigma$ level. The statistical error-in-the-mean is an underestimate of the total uncertainty, however. The CTI correction may be off by as much as 25%; we conservatively estimate a $1\text{-}\sigma$ systematic error of $\pm 0.58 \text{ mas yr}^{-1}$ in the readout direction, oriented 34.17° east of north.

We transform HVS3’s observed heliocentric motion into the Galactic rest frame assuming a circular velocity of 220 km s^{-1} and a solar motion of $(U, V, W) = (11.1, 12.24, 7.25) \text{ km s}^{-1}$ per Schönrich et al. (2010). The Galactocentric velocity components are thus $(U, V, W) = (-119, -400, -355) \text{ km s}^{-1}$.

3. TRAJECTORY

We calculate the trajectory of HVS3 with respect to the Milky Way and LMC using the Kenyon et al. (2008) three-component potential model. This model uses a circular velocity of 220 km s^{-1} at the solar radius and assumes a total stellar mass of $4.4 \times 10^{10} M_\odot$ and a dark matter halo virial mass of $1 \times 10^{12} M_\odot$ with a scale radius of 20 kpc. The details of the mass distribution are

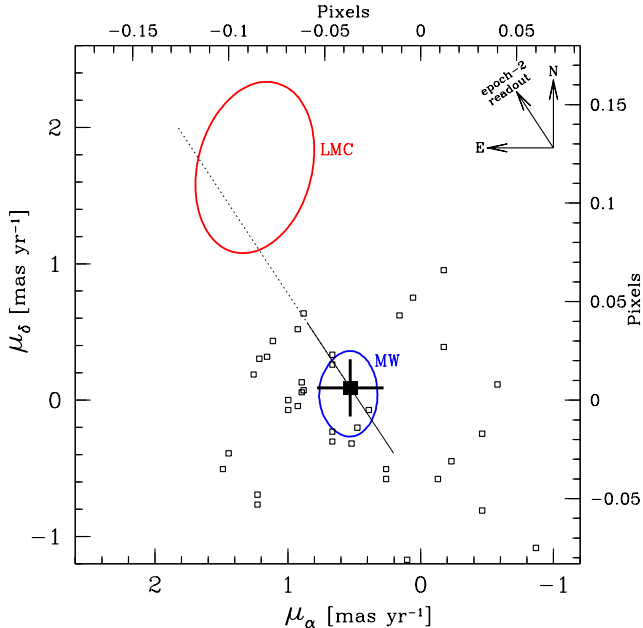


Figure 2. Mean proper motion of HVS3 (*solid square*) and the distribution of proper motions (*open squares*) measured from the individual epoch-1 and epoch-2 images. The $1\text{-}\sigma$ statistical uncertainty (*plus sign*) and systematic uncertainty (*solid line*) are indicated, as well as the full CTI correction (*dotted line*). We also show the locus of proper motions with trajectories passing within 8 kpc of the Milky Way center (*lower ellipse*) and within 3 kpc of the LMC center (*upper ellipse*) at the time of pericenter passage. HVS3’s velocity vector points from the Milky Way; an origin from the center of the LMC is ruled out at $3\text{-}\sigma$ (systematic).

not very important because HVS3 spends most its time traveling through the outer halo; a cross-check using the Gnedin et al. (2005) potential yields identical results.

We account for the changing position of the LMC in all of our calculations. We assume the LMC currently has the location and line-of-sight velocity from van der Marel (2001) and the proper motion from Kallivayalil et al. (2006). We establish the LMC’s location versus time by computing the LMC’s orbit in our potential model. We then assign the LMC a point mass of $2 \times 10^{10} M_{\odot}$ in our calculations.

To put the proper motion of HVS3 in context, we begin by computing trajectories for the full range of possible proper motions. The elliptical contours in Figure 2 show the locus of proper motions whose outbound trajectories pass within 8 kpc of the Milky Way center (lower ellipse) and within 3 kpc of the LMC center (upper ellipse) at the time of pericenter passage. We chose 3 kpc for the LMC because this radius encompasses the extent of the LMC bar, 85% of the LMC’s observed young stellar objects (Gruendl & Chu 2009), and all of the young clusters proposed by Gualandris & Portegies Zwart (2007) for the origin of HVS3.

Figure 2 shows that the full space motion of HVS3 points directly from the Milky Way. The Galactic center and most of the disk fall within the proper motion $1\text{-}\sigma$ systematic error bar. An LMC origin, on the other hand, requires a large, northerly tangential motion ruled out at $3\text{-}\sigma$ (systematic) or better.

Next we consider the trajectory of HVS3 in physical space. Figure 3 plots the present location and computed trajectory for both HVS3 and the LMC in a Cartesian co-

Table 1
HVS3 OBSERVED PARAMETERS

Parameter	Value	Ref
RA (J2000)	4:38:12.8	1
Dec (J2000)	−54:33:12	1
v_{helio} (km s $^{-1}$)	723 ± 3	1,2,3
V (mag)	16.36 ± 0.04	2
$B - V$ (mag)	-0.23 ± 0.03	2
T_{eff} (K)	23000 ± 1000	3
$\log g$ (cgs)	3.95 ± 0.10	3
$v \sin i$ (km s $^{-1}$)	55 ± 2	2,3
M (M_{\odot})	9.1 ± 0.8	3
d_{helio} (kpc)	61 ± 9	3
μ_{α} (mas yr $^{-1}$)	$+0.53 \pm 0.25(\text{stat}) \pm 0.33(\text{sys})$	
μ_{δ} (mas yr $^{-1}$)	$+0.09 \pm 0.21(\text{stat}) \pm 0.48(\text{sys})$	

References. — (1) Edelmann et al. (2005); (2) Bonanos et al. (2008); (3) Przybilla et al. (2008a)

Note. — All errors are $1\text{-}\sigma$

ordinate system centered on the Milky Way. Arrowheads indicate the present direction of motion. 23 Myr ago, HVS3 passed within 13 kpc of the LMC. For comparison, the LMC’s outermost stars and star clusters are 10 kpc distant from the LMC (van der Marel 2001; Bica et al. 1996). 98 Myr ago, HVS3 crossed the Galactic plane. McMillan & Binney (2010) argue that the Sun’s circular velocity should be 240 km s^{-1} at $R_0=8$ kpc; this changes the flight time and Galactic plane-crossing location of HVS3 by <3 Myr and <1 kpc, respectively.

To establish where HVS3 most likely crossed the Galactic plane, we propagate the measurement uncertainties (Table 1) through a Monte Carlo calculation. We assume that the uncertainties are Gaussian distributed, and calculate trajectories for 1 million random draws of HVS3’s distance, radial velocity, and proper motion. Figure 3 shows the resulting distribution of Galactic plane-crossing locations: the ellipses show the 1- , 2- , and $3\text{-}\sigma$ levels of the distribution, considering all the errors simultaneously. The ± 9 kpc distance uncertainty is a dominant source of error. The origin of HVS3 is formally consistent with both the Galactic center and the Galactic disk based on its trajectory alone.

4. STELLAR NATURE

Bonanos et al. (2008) and Przybilla et al. (2008a) independently measure solar Fe and half-solar C, N, O, Mg, Si abundances for HVS3. The observed abundance pattern is consistent with an LMC or a Milky Way outer disk origin, however the pattern is also consistent with a Galactic center origin within the 1- to $2\text{-}\sigma$ uncertainties (Przybilla et al. 2008a). If HVS3 is a blue straggler, on the other hand, it is unclear what abundance pattern we should expect. Fortunately, the kinematics paint a clearer picture.

Bonanos et al. (2008) and Przybilla et al. (2008a) find that the surface gravity, effective temperature, and rotation of HVS3 are those of a $9 M_{\odot}$ main-sequence star with a lifetime of $\simeq 20$ Myr. This lifetime, combined with its 98 ± 17 Myr flight time from the Milky Way, requires that HVS3 is a blue straggler.

Blue stragglers are ubiquitous in globular clusters, open clusters, and in the “field” of the Milky Way: half of all A-type stars in the stellar halo are main-sequence blue stragglers (e.g. Wilhelm et al. 1999; Preston & Sneden

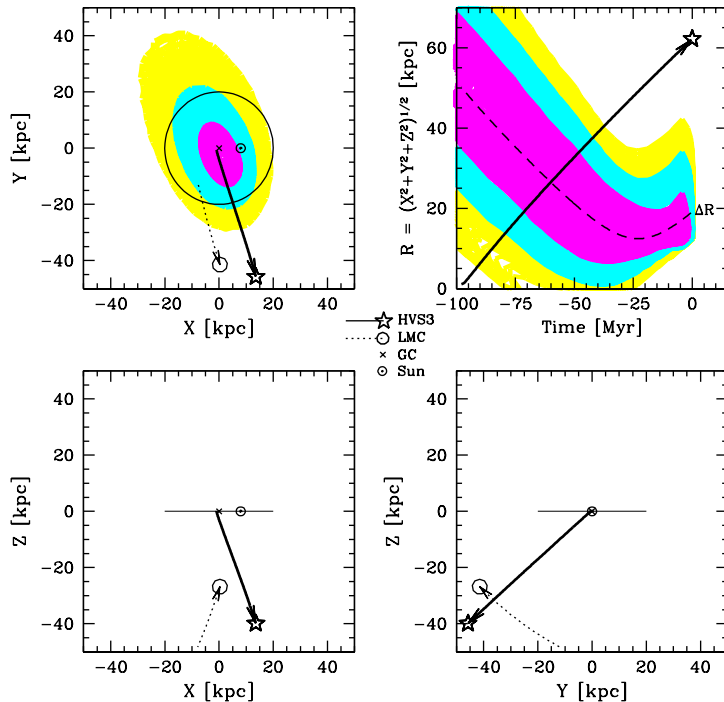


Figure 3. Trajectory of HVS3 (*solid line*) and LMC (*dotted line*) over the past 98 Myr plotted in physical Cartesian coordinates centered on the Milky Way. Symbols mark the present position of HVS3 (*star*), the LMC (*open circle*), and the Sun (\odot). Arrowheads indicate the present direction of motion. The Milky Way disk is indicated by a 20 kpc radius circle; the LMC is indicated by a 3 kpc radius circle. The likelihood of HVS3’s Galactic plane-crossing is plotted for 1- σ (*magenta ellipse*), 2- σ (*cyan ellipse*), and 3- σ (*yellow ellipse*) levels in the upper right panel. The separation of HVS3 and the center of the LMC (*dashed line*) and the 1- σ (*magenta band*), 2- σ (*cyan band*), and 3- σ (*yellow band*) distribution of separations are plotted in the upper right panel. All errors, statistical and systematic, are considered simultaneously.

2000; Brown et al. 2008). Blue stragglers probably form by either binary mass transfer or mergers (Bailyn 1995). The resulting blue straggler then evolves quite normally as a main-sequence star of higher mass (Sills et al. 2009). For HVS3, the implication is that a pair of $4.5 M_{\odot}$ stars, with main-sequence lifetimes of 160 Myr (Girardi et al. 2002), evolved and merged during their 98 Myr flight time from the Milky Way.

The only alternative is that HVS3 is a post main-sequence star (Demarque & Virani 2007). However, Edelmann et al. (2005) show that HVS3’s $\log g$ is too low for its temperature, and its rotation too large, for it to be a horizontal branch (HB) star. Alternatively, HVS3 could be an AGB-manqué star, a post-HB star with too little hydrogen to reach the asymptotic giant branch (AGB), or a post-AGB star. Evolutionary tracks show that AGB-manqué and post-AGB stars spend 10^5 yrs at HVS3’s T_{eff} and $\log g$, with approximately one-tenth the luminosity of a main-sequence star (Dorman et al. 1993). Thus in both the AGB-manqué and post-AGB scenarios, HVS3’s lifetime constraint is relaxed but the star is *still approaching* the LMC. The AGB-manqué and post-AGB interpretations are problematic, however. HVS3 rotates too rapidly for such an evolved star. In addition, the joint probability of finding a star in a rare evolutionary phase that lasts $<10^{-5}$ of the star’s lifetime and that is also a HVS ($\sim 10^{-7}$ of Milky Way stars are HVSs) is very small. We find no compelling reason to contradict the observed main-sequence nature of HVS3, and assume that HVS3 is a blue straggler.

5. ORIGIN

Because HVS3 is a blue straggler with a main-sequence lifetime less than its flight time, it must have been ejected from the Milky Way as a binary system that subsequently merged during its flight.

It is difficult, however, to eject a binary with the necessary velocity from the disk of the Milky Way. The trajectory of HVS3 crosses the disk at 820 km s^{-1} . In comparison, a pair of $4.5 M_{\odot}$ stars with $3.4 R_{\odot}$ radii and separated by $8.5 R_{\odot}$ (their Roche-lobe overflow separation) have an orbital velocity of 320 km s^{-1} . Thus a 820 km s^{-1} kick exceeds by 2.5 times the orbital velocity of a pair of $4.5 M_{\odot}$ stars in a compact binary, and it also exceeds the 710 km s^{-1} escape velocity from the surface of a $4.5 M_{\odot}$ star. Thus any stellar dynamical mechanism that might have ejected the progenitor binary from the disk would have destroyed the progenitor.

Ejecting a binary at 820 km s^{-1} likely requires a more massive and compact object, such as a MBH. Two proposed mechanisms are: a binary MBH that ejects stellar binaries as HVSs (Lu et al. 2007), and a single MBH that ejects binaries by triple disruption (Perets 2009b).

Provided that the separation between a pair of MBHs is substantially larger than the tidal disruption distance of binary stars, Lu et al. (2007) estimate that a binary MBH ejects $>50\%$ of incoming binaries with $v > 900 \text{ km s}^{-1}$. They predict that HVS binaries comprise 3-5% of all HVSs. Sesana et al. (2009) find similar HVS binary frequencies based on more detailed simulations, although

Perets (2009a) argues this may be an overestimate. Interestingly, the 16-19 HVSs observed to date are consistent with finding 1 HVS binary. In the context of HVS3, the binary MBH scenario implies that an IMBH in-spiraled into the Milky Way’s central MBH about 100 Myr ago.

Perets (2009b), on the other hand, argues that HVS binary ejection is the natural consequence of a single MBH disrupting triple stars. For context, essentially all O and B stars are observed in binaries, and half of the binaries are equal mass twins (Pinsonneault & Stanek 2006). Hierarchical triples are stable if the outer binary has a much larger separation than the inner compact binary; Perets (2009b) shows that a MBH interaction can disrupt the outer binary while the inner binary remains bound. Perets estimates that 3-5% of HVS ejections will be HVS binaries from disrupted triples. Because the ejected binaries are compact, most will undergo type-A mass transfer and merge. Thus the Perets (2009b) triple disruption mechanism also explains the blue-straggler nature of HVS3.

If HVSs originate from the Galactic center, it appears inevitable that some HVSs will be binaries. We estimate the likelihood of HVS3 being a (former) binary by looking at the complete survey of Brown et al. (2007b), who infer 96 ± 20 $3-4 M_{\odot}$ HVSs are located within 100 kpc of the Galactic center. If 5% of HVS ejections are binaries, then there should be 5 HVS binaries containing $\simeq 4 M_{\odot}$ stars. Assuming these (necessarily compact) binaries all evolve to form a $\simeq 8 M_{\odot}$ blue straggler with a lifetime of 30 Myr, we expect 30 Myr / 160 Myr = 20% in the blue-straggler phase, or about 1 star on average. We conclude that the stellar nature and kinematics of HVS3 are consistent with it being an ejected HVS binary as proposed by Lu et al. (2007) and Perets (2009b).

6. CONCLUSION

We measure the proper motion of HVS3 and find that its velocity vector points from the Milky Way. An origin from the center of the LMC is ruled out at $3-\sigma$ (systematic). Because HVS3’s travel time from the Milky Way exceeds its main-sequence lifetime, it must be a blue straggler whose progenitor was ejected from the Milky Way as a binary system. The star’s abundance pattern is ambiguous, but the kinematics are clear. The finite size of stars imposes a velocity constraint that rules out a disk ejection. Combining the observed trajectory, stellar nature, and required initial velocity, we conclude that HVS3 is a former binary ejected by the MBH in the Galactic center. In the future, a 3rd epoch of imaging will greatly improve the proper motion constraint: doubling the time baseline will halve the internal error, and matching the image orientation will reduce the systematic error by 67%.

We thank Andy Gould, Hagai Perets, and the anonymous referee for helpful comments. Support for this research was provided by NASA through grants GO-10824 and GO-11782 from the Space Telescope Science Institute, which is operated by the Association of Universities for Research in Astronomy, Inc., under NASA contract NAS5-26555. This research makes use of NASA’s Astrophysics Data System Bibliographic Services. This work was supported in part by the Smithsonian Institution.

Facilities: HST (ACS)

REFERENCES

- Anderson, J. & King, I. R. 2006, “PSFs, Photometry, and Astronomy for the ACS/WFC”, Tech. rep., STScI
- Anderson, J. W. & Bedin, L. R. 2010, PASP, accepted
- Bailyn, C. D. 1995, ARA&A, 33, 133
- Bica, E., Claria, J. J., Dottori, H., Santos, Jr., J. F. C., & Piatti, A. E. 1996, ApJS, 102, 57
- Bonanos, A. Z., López-Morales, M., Hunter, I., & Ryans, R. S. I. 2008, ApJ, 675, L77
- Brown, W. R., Beers, T. C., Wilhelm, R., Allende Prieto, C., Geller, M. J., Kenyon, S. J., & Kurtz, M. J. 2008, AJ, 135, 564
- Brown, W. R., Geller, M. J., & Kenyon, S. J. 2009, ApJ, 690, 1639
- Brown, W. R., Geller, M. J., Kenyon, S. J., & Kurtz, M. J. 2005, ApJ, 622, L33
- . 2006a, ApJ, 640, L35
- . 2006b, ApJ, 647, 303
- Brown, W. R., Geller, M. J., Kenyon, S. J., Kurtz, M. J., & Bromley, B. C. 2007a, ApJ, 660, 311
- . 2007b, ApJ, 671, 1708
- Demarque, P. & Virani, S. 2007, A&A, 461, 651
- Dorman, B., Rood, R. T., & O’Connell, R. W. 1993, ApJ, 419, 596
- Edelmann, H., Napiwotzki, R., Heber, U., Christlieb, N., & Reimers, D. 2005, ApJ, 634, L181
- Fuentes, C. I., Stanek, K. Z., Gaudi, B. S., McLeod, B. A., Bogdanov, S., Hartman, J. D., Hickox, R. C., & Holman, M. J. 2006, ApJ, 636, L37
- Ghez, A. M. et al. 2008, ApJ, 689, 1044
- Gillessen, S., Eisenhauer, F., Trippe, S., Alexander, T., Genzel, R., Martins, F., & Ott, T. 2009, ApJ, 692, 1075
- Ginsburg, I. & Loeb, A. 2006, MNRAS, 368, 221
- Girardi, L. et al. 2002, A&A, 391, 195
- Gnedin, O. Y., Gould, A., Miralda-Escudé, J., & Zentner, A. R. 2005, ApJ, 634, 344
- Gould, A. & Quillen, A. C. 2003, ApJ, 592, 935
- Gruendl, R. A. & Chu, Y. 2009, ApJS, 184, 172
- Gualandris, A. & Portegies Zwart, S. 2007, MNRAS, 376, L29
- Gvaramadze, V. V., Gualandris, A., & Portegies Zwart, S. 2008, MNRAS, 385, 929
- . 2009, MNRAS, 396, 570
- Heber, U., Edelmann, H., Napiwotzki, R., Altmann, M., & Scholz, R.-D. 2008, A&A, 483, L21
- Hills, J. G. 1988, Nature, 331, 687
- Hirsch, H. A., Heber, U., O’Toole, S. J., & Bresolin, F. 2005, A&A, 444, L61
- Irrgang, A., Przybilla, N., Heber, U., Fernanda Nieva, M., & Schuh, S. 2010, ApJ, 711, 138
- Kallivayalil, N., van der Marel, R. P., Alcock, C., Axelrod, T., Cook, K. H., Drake, A. J., & Geha, M. 2006, ApJ, 638, 772
- Kenyon, S. J., Bromley, B. C., Geller, M. J., & Brown, W. R. 2008, ApJ, 680, 312
- López-Morales, M. & Bonanos, A. Z. 2008, ApJ, 685, L47
- Lu, Y., Yu, Q., & Lin, D. N. C. 2007, ApJ, 666, L89
- Mahmud, N. & Anderson, J. 2008, PASP, 120, 907
- McMillan, P. J. & Binney, J. J. 2010, MNRAS, 402, 934
- Perets, H. B. 2009a, ApJ, 690, 795
- . 2009b, ApJ, 698, 1330
- Perets, H. B., Hopman, C., & Alexander, T. 2007, ApJ, 656, 709
- Pinsonneault, M. H. & Stanek, K. Z. 2006, ApJ, 639, L67
- Preston, G. W. & Sneden, C. 2000, AJ, 120, 1014
- Przybilla, N., Nieva, M. F., Heber, U., Firnstein, M., Butler, K., Napiwotzki, R., & Edelmann, H. 2008a, A&A, 480, L37
- Przybilla, N., Nieva, M. F., Tillich, A., Heber, U., Butler, K., & Brown, W. R. 2008b, A&A, 488, L51
- Schönrich, R., Binney, J., & Dehnen, W. 2010, MNRAS, 403, 1829
- Sesana, A., Madau, P., & Haardt, F. 2009, MNRAS, 392, L31
- Sills, A., Karakas, A., & Lattanzio, J. 2009, ApJ, 692, 1411
- Tillich, A., Przybilla, N., Scholz, R., & Heber, U. 2009, A&A, 507, L37
- van der Marel, R. P. 2001, AJ, 122, 1827
- Wilhelm, R. et al. 1999, AJ, 117, 2329
- Yu, Q. & Tremaine, S. 2003, ApJ, 599, 1129